



## Band-gap tuning at the strong quantum confinement regime in magnetic semiconductor EuS thin films

Panagiotis Pouloupoulos, Björn Lewitz, Andreas Straub, Spiridon D. Pappas, Sotirios A. Droulias, Sotirios Baskoutas, and Paul Fumagalli

Citation: *Applied Physics Letters* **100**, 211910 (2012); doi: 10.1063/1.4720167

View online: <http://dx.doi.org/10.1063/1.4720167>

View Table of Contents: <http://scitation.aip.org/content/aip/journal/apl/100/21?ver=pdfcov>

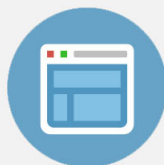
Published by the [AIP Publishing](http://www.aip.org)

---



## Re-register for Table of Content Alerts

Create a profile.



Sign up today!



## Band-gap tuning at the strong quantum confinement regime in magnetic semiconductor EuS thin films

Panagiotis Pouloupoulos,<sup>1,2,a)</sup> Björn Lewitz,<sup>1</sup> Andreas Straub,<sup>1</sup> Spiridon D. Pappas,<sup>3</sup> Sotirios A. Droulias,<sup>2</sup> Sotirios Baskoutas,<sup>2</sup> and Paul Fumagalli<sup>1</sup>

<sup>1</sup>*Institut für Experimentalphysik, Freie Universität Berlin, Arnimallee 14, D-14195 Berlin-Dahlem, Germany*

<sup>2</sup>*Materials Science Department, University of Patras, 26504 Patras, Greece*

<sup>3</sup>*School of Engineering, Engineering Science Department, University of Patras, 26504 Patras, Greece*

(Received 5 March 2012; accepted 6 May 2012; published online 23 May 2012)

Ultraviolet-visible absorption spectra of nanoscaled EuS thin films reveal a blue shift of the energy between the top-valence and bottom-conduction bands. This band-gap tuning changes smoothly with decreasing film thickness and becomes significant below the exciton Bohr diameter  $\sim 3.5$  nm indicating strong quantum confinement effects. The results are reproduced in the framework of the potential morphing method in Hartree Fock approximation. The large values of the effective mass of the holes, due to localization of the EuS  $f$ -states, limit the blue shift to about 0.35 eV. This controllable band-gap tuning of magnetic semiconductor EuS renders it useful for merging spintronics and optoelectronics. © 2012 American Institute of Physics. [<http://dx.doi.org/10.1063/1.4720167>]

Europium sulfide (EuS) is a natural ferromagnetic semiconductor. As compared to other magnetic semiconductors, it presents the advantage that spin-polarized electrons are created within the semiconductor. The disadvantage of it is the low Curie temperature of only  $\sim 16.6$  K. However, by increasing the Curie temperature of EuS, e.g., due to proximity with Cobalt, EuS may become an important candidate for technological applications in the era of magnetic semiconductors and spintronics.<sup>1–4</sup> As a semiconductor, it has an optical band gap  $E_g \sim 1.65$  eV as revealed by optical absorption spectra which show a broad absorption peak with onset at  $\sim 1.65$  eV and maximum at  $\sim 2.33$  eV. The absorption peak is attributed to transitions between the  $4f^7(^8S_{7/2})$  to  $4f^6(^7F_J)5d(t_{2g})$  electronic states.<sup>5,6</sup> Controllable tuning of  $E_g$  of EuS may render EuS useful for merging spintronics and optoelectronics, as, for example, in spin-controlled light emitting diodes or vertical-cavity surface-emitting lasers.<sup>7</sup> The band gap depends strongly on the particle size (quantum dots) or thin film thickness (quantum wells) and, often, it increases as the size or thickness decreases, i.e., a blue shift of the band gap occurs due to quantum confinement effects.<sup>8–11</sup> Recent works on EuS nanoparticles synthesized via chemical methods report either no quantum confinement effects<sup>12</sup> or a small blue shift of the first absorption maximum in the weak quantum confinement regime, i.e., when the particle diameter approaches the exciton Bohr radius of the quantum dot.<sup>13</sup> However, a systematic evolution of the blue shift with quantum dot size was not provided and the maximum blue shift reported was  $\sim 0.1$  eV.<sup>14</sup>

In this work, we demonstrate a systematic tuning of the band gap with film thickness due to quantum confinement in EuS thin films. The band gap increases in a smooth way reaching for the thinnest film of 2 nm a maximum blue shift of 0.35 eV in the strong quantum-confinement regime. Such a strong blue shift due to quantum confinement effects has

not been demonstrated previously for Europium Sulfide. Theoretical calculations based on the potential morphing method (PMM) in the Hartree Fock approximation<sup>9,15–17</sup> provide sets of blue shifts of the excitonic binding energy for various combinations of the electron and hole effective masses of EuS. A fair agreement is observed between theory and experiment. The large hole effective mass due to the localization of the  $4f$  states of EuS<sup>18</sup> seems to be a limiting parameter in the increase of the blue shift to very large values. Our combined experimental and theoretical work provides an insight to quantum-confinement effects and to tailoring of the blue shift of the band gap in nanoscaled systems.

EuS thin films with thickness 2–83 nm were deposited by e-beam sublimation on quartz and on the native oxide of Si(100) wafers in an ultrahigh vacuum (UHV) chamber (BALZERS). The base pressure of the chamber was  $4 \times 10^{-9}$  mbars. EuS powder of high purity was sublimed from a tungsten crucible. A weak e-beam of 25 mA had to be scanned across the surface of the powder in order to get a deposition rate of 0.05 nm/s. The material sublimates directly from the target. Deposition temperature was about 250 °C to promote better crystallinity. No capping layer was used as EuS is stable in air. The film thickness was measured with a precalibrated quartz balance.

The thickness evaluation and structural characterization of the films were mainly performed with the help of x-ray diffraction (XRD) experiments recorded at small or high angles using a standard powder diffractometer (Berthold) with Ni- and Co-filtered  $\text{CuK}\alpha_1$  radiation ( $\lambda = 0.154059$  nm). Figure 1(a) plots a small-angle x-ray reflectivity (XRR) pattern (open symbols) for a thin EuS film grown on the native amorphous oxide of a Si(100) wafer. The appearance of many Kiessig fringes in the XRR pattern indicates high homogeneity in the film thickness and very small surface roughness. A rigorous analysis of the pattern was done via the GenX code.<sup>19</sup> The roughness profile in the simulations of the experimental data is introduced as a sinusoidal modulation of the layer thickness. The final calculated roughness

<sup>a)</sup>Author to whom correspondence should be addressed. Electronic mail: pouloupoulos@zedat.fu-berlin.de. Tel. (+49) 30 838 56078. Fax (+49) 30 838 56299.

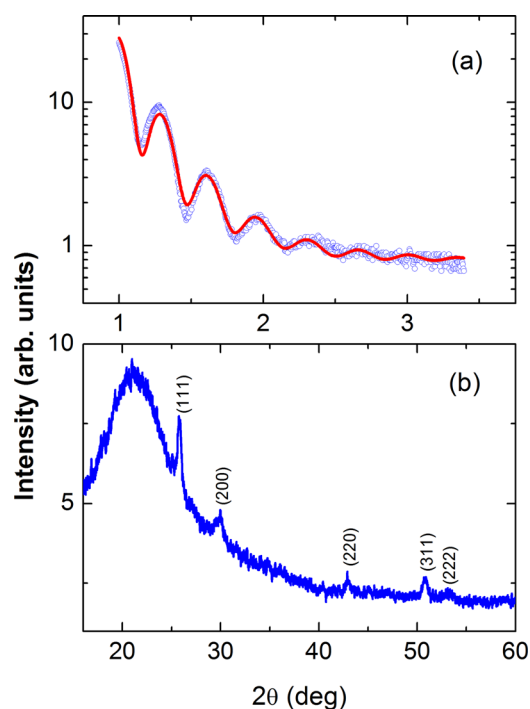


FIG. 1. (a) Small-angle XRR pattern (open symbols) for a thin EuS film grown on the native amorphous oxide of a Si(100) wafer. The fitted pattern using the GenX code is also shown (continuous line). (b) X-ray diffraction pattern of a 83 nm thick EuS film grown on quartz. The film is polycrystalline with moderate {111} texture.

values correspond to the root-mean-square (rms) value of this sinusoidal modulation. The GenX-fitted pattern is also included in Fig. 1(a) (continuous line). From the fitting, one determines a EuS film thickness  $d_{\text{Cu}} = 25.56$  nm with rms roughness  $R_{\text{rms}} = 0.581$  nm. The model which is used in the simulation procedure includes also a native  $\text{Si}_2\text{O}$  layer with thickness 1.66 nm and rms roughness 0.31 nm.

In Fig. 1(b), we show a high-angle XRD pattern from the 83 nm EuS film grown on quartz. The amorphous substrate results in a very broad background mainly at about  $22^\circ$ . The diffraction positions reveal a polycrystalline EuS film with moderate {111} texture. From the positions of the Bragg peaks, one may evaluate with the help of Bragg's law a lattice constant of 0.5962 nm, which is within the experimental accuracy equal to the one of bulk EuS, 0.5968 nm.<sup>20</sup>

The ultraviolet (UV)-visible spectra of the EuS films on quartz were recorded at room temperature in transmission geometry with the help of a Perkin Elmer  $\Lambda$ -35 UV-visible spectrometer in a wavelength range of 200–1100 nm. Quartz was used because it is optically transparent within the measurement wavelength range. All samples were measured immediately after preparation. However, measurements performed after about 1 month were identical revealing the stability of the materials under air exposure.

Figure 2 depicts the normalized light absorption spectrum for a 7.5 nm thick EuS film (open symbols). The normalization process is explained in Ref. 21. The spectrum is similar to the one of thick EuS films (50–300 nm).<sup>5,6</sup> The dashed curves represent the deconvoluted absorption bands of the optical absorption spectra with their centers nearby the positions of the optical transitions derived by Güntherodt.<sup>6</sup> A Gaussian broadening was considered due to the fact that our

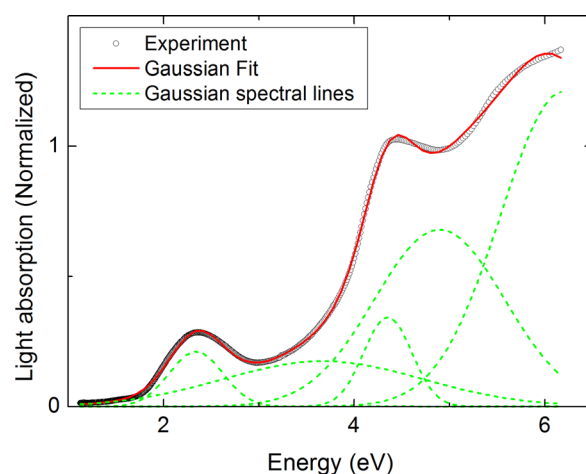


FIG. 2. Normalized optical (light) absorption spectrum for a 7.5 nm thick EuS film (open symbols). The solid line is the result of a fitting taking into consideration absorption lines (dashed lines) according to the optical transition scheme of Güntherodt.<sup>6</sup> A Gaussian shape was considered due to thermal broadening.

measurements were performed at room temperature. The solid line is the sum of the dashed lines and represents the fitted experimental spectrum. With this analysis, one may determine accurately the positions of the maximum of the broadened absorption lines.

Figure 3 depicts the normalized light absorption spectra for three EuS films with thickness between 3 and 10 nm. The signal-to-noise ratio is high even for the thinnest sample. As the film thickness decreases, a smoothing of the absorption peaks is exhibited. The first absorption peak is shown to decrease in amplitude and move to higher energies with decreasing film thickness, as the inset of Fig. 3 clearly reveals. At a film thickness of 2 nm, the first absorption peak becomes very small. Below this thickness, the determination of any characteristic feature is meaningless. This observation may have to do with a decrease of the crystal-field splitting due to partial amorphization of the films at very small thickness. It is obvious, even by eye inspection, that the absorption peak shows a blue shift which becomes significant for

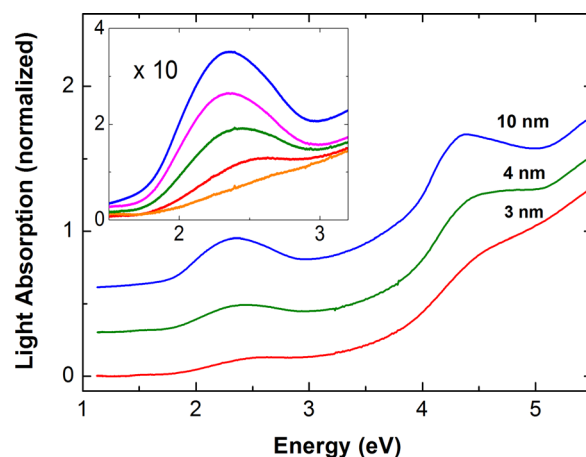


FIG. 3. Normalized optical (light) absorption spectra for thin EuS films fabricated on quartz. The spectra have been vertically shifted for clarity. The thickness of the films is marked on each absorption spectrum. In the inset, we show enlarged the first absorption peak for 5 samples. The thickness from the top to the bottom is 10, 5.5, 4, 3, and 2 nm.

the three thinnest films with thickness between 2 and 4 nm. This effect may be qualitatively understood if one considers that the film thickness is comparable or smaller than the exciton Bohr diameter for the onset of quantum confinement effects. Indeed, if the effective electron mass  $m_e^*$  for EuS is  $0.3m_0$ ,<sup>22</sup> where  $m_0$  is the free electron mass and the optical dielectric constant  $\epsilon \sim 10$ ,<sup>23</sup> then the exciton Bohr diameter for EuS can be calculated  $\sim 3.5$  nm.

For a quantitative analysis of the blue shift of the absorption peak, the onset of it, which corresponds to  $E_g \sim 1.65$  eV for thick EuS films,<sup>5</sup> is not the best selection because it is not well-defined, see inset of Fig. 3. However, since it is very common in literature to be estimated with the help of the Tauc method, see, e.g., Ref. 12, we applied this method to our experimental spectra and the blue shifts with decreasing film thickness appear in Fig. 4 as half filled circles. As we have shown in previous work,<sup>9,21</sup> in order to have a precise determination of the energy position of the absorption edge (usually with relative error bars 0.02 eV), it is better to consider the edge position to be determined by the maximum of the first derivative or, equivalently, by the zeroing of the second derivative of the optical absorption with respect to the energy. Figure 4 presents the blue shift of the edge position (filled circles with error bars). We see that the two experimental data sets coincide within the error bars. The blue shift increases as the film thickness decreases and becomes quite significant  $\sim 0.35$  eV at 2 nm. We made also an effort to measure the shift in the energy position of the first absorption peak at about 2.33 eV, i.e., the position of the first band originating from the crystal field splitting. This can be determined by deconvolution of the absorption spectra, as shown in Fig. 2. This position is also clearly identified. The results for the blue shift are identical within the experimental error bar with the ones for the band gap appearing in Fig. 4.

In Fig. 4, we have also introduced calculations with the help of the potential morphing method. This method was originally developed to calculate quantum-confinement effects in quantum dots but can also be applied for thin films.<sup>21</sup> In order to investigate the EuS system, we assume

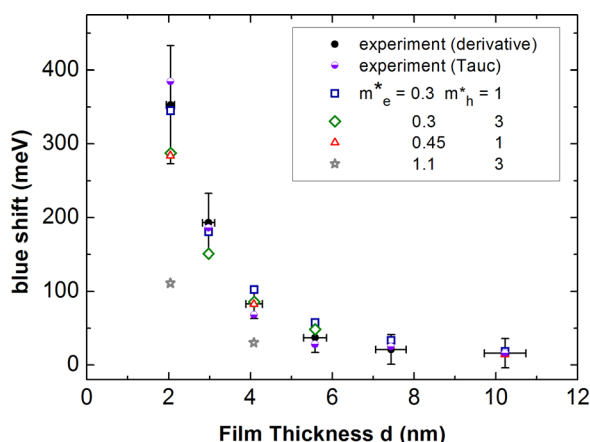


FIG. 4. Experimentally determined blue shift of the band gap energy for EuS films with thickness  $d$  between 2 and 10 nm by the derivative method (filled) or the Tauc method (half-filled circles). The open symbols represent calculated results with the help of the potential morphing method for various combinations of the electron and hole effective masses in  $m_0$  units, as indicated. Not all open symbols have been plotted for better readability.

that the substrate is transparent  $\text{SiO}_2$  with  $E_g \sim 8.9$  eV. For the electron effective mass  $m_e^*$ , we have tried all the values provided in literature, that is  $0.3 m_0$ ,<sup>22</sup>  $0.45 m_0$ ,<sup>24</sup> and  $1.1 m_0$ .<sup>25</sup> The hole effective mass  $m_h^*$  must be considered much larger than the  $m_e$  value.<sup>24</sup> Therefore, acceptable couples of values for  $m_e^*$  and  $m_h^*$  are the ones which make practically the exciton reduced mass  $\mu$  equal to  $m_e^*$ , see, for example, the discussion in Ref. 13. In this heavy hole approximation, the corresponding values for the exciton Bohr radius are 1.7 nm,<sup>22</sup> 1.2 nm,<sup>24</sup> and 0.5 nm.<sup>25</sup> Our calculations show a very good agreement between experiment and theory for  $m_e^* = 0.3 m_0$  and  $m_h^* = 1 m_0$ . Fair agreement is also observed for  $m_e^* = 0.3 m_0$  and  $m_h^* = 3 m_0$  and similarly for  $m_e^* = 0.45 m_0$  and  $m_h^* = 1 m_0$ . On the other hand for  $m_e^* = 1.1 m_0$  and  $m_h^* = 3 m_0$ , the theory fails to reproduce the experimental results. From the aforementioned four couples of  $m_e^*$  and  $m_h^*$ , the one which describe fairly well the experiment and the condition  $m_h^* \gg m_e^*$  is the couple  $m_e^* = 0.3 m_0$  and  $m_h^* = 3 m_0$ . Therefore, the comparison between the theoretical and the experimental results shows good agreement and indicates that the observed significant blue shift of the first absorption peak of EuS can be attributed to the presence of strong quantum-confinement effects for film thickness which is smaller than the exciton Bohr diameter of  $\sim 3.5$  nm for the EuS.

In summary, we have demonstrated a blue shift of the band gap of EuS thin films as the film thickness decreases. The blue shift becomes significant in the strong quantum-confinement regime below 4 nm of film thickness and reaches a maximum value of 0.35 eV for a 2 nm thick EuS film. The results can be calculated fairly well with the help of the potential morphing method. Tuning of the band gap of the magnetic semiconductor EuS may render this material useful for combining spintronic and optoelectronic applications.<sup>26</sup>

P.P. thanks the Center for International Cooperation (C.I.C.) of the Freie Universität Berlin for partial financial support and the Institute for Experimental Physics, Freie Universität Berlin for the great hospitality. Grant Karatheodori2009, Nr. C.905 and Grant Karatheodori2010-2013, Nr. D.207 of the Research Committee of the University of Patras are also acknowledged.

<sup>1</sup>P. Fumagalli, A. Schirmeisen, and R. J. Gambino, *Phys. Rev. B* **57**, 14294 (1998).

<sup>2</sup>S. A. Wolf, D. D. Awschalom, R. A. Buhrman, J. M. Daughton, S. von Molnár, M. L. Roukes, A. Y. Chtchelkanova, and D. M. Treger, *Science* **294**, 1488 (2001).

<sup>3</sup>I. Žutić, J. Fabian, and S. Das Sarma, *Rev. Mod. Phys.* **76**, 323 (2004).

<sup>4</sup>C. Müller, H. Lippitz, J. J. Paggel, and P. Fumagalli, *J. Appl. Phys.* **99**, 073904 (2006).

<sup>5</sup>G. Güntherodt, J. Schoenes, and P. Wachter, *J. Appl. Phys.* **41**, 1083 (1970).

<sup>6</sup>G. Güntherodt, P. Wachter, and D. M. Imboden, *Phys. kondens. Mater.* **12**, 292 (1971).

<sup>7</sup>S. Hövel, N. C. Gerhardt, C. Brenner, M. R. Hofmann, F.-Y. Lo, D. Reuter, A. D. Wieck, E. Schuster, and W. Keune, *Phys. Status Solidi A* **204**, 500 (2007).

<sup>8</sup>K. K. Nanda, F. E. Kruijs, and H. Fissan, *Nano Lett.* **1**, 605 (2001).

<sup>9</sup>S. Baskoutas, P. Pouloupoulos, V. Karoutsos, M. Angelakeris, and N. K. Flevaris, *Chem. Phys. Lett.* **417**, 461 (2006).

<sup>10</sup>D. Z. Sun and H. J. Sue, *Appl. Phys. Lett.* **94**, 253106 (2009).

<sup>11</sup>T. Li, F. Gygi and G. Galli, *Phys. Rev. Lett.* **107**, 206805 (2011).

- <sup>12</sup>V. M. Huxter, T. Mirkovic, P. S. Nair, and G. D. Scholes, *Adv. Mater.* **20**, 2439 (2008).
- <sup>13</sup>M. D. Regulacio, S. Kar, E. Zuniga, G. Wang, N. R. Dollahon, G. T. Yee and S. L. Stoll, *Chem. Mater.* **20**, 3368 (2008).
- <sup>14</sup>D. S. Koktysh, S. Somarajan, W. He, M. A. Harrison, S. A. McGill and J. H. Dickerson, *Nanotechnology* **21**, 415601 (2010).
- <sup>15</sup>S. Baskoutas and A. F. Terzis, *J. Appl. Phys.* **99**, 013708 (2006); S. Baskoutas, E. Paspalakis, and A. F. Terzis, *Phys. Rev. B* **74**, 153306 (2006).
- <sup>16</sup>S. Baskoutas, A. F. Terzis, and W. Schommers, *J. Comput. Theor. Nanosci.* **3**, 269 (2006).
- <sup>17</sup>S. Baskoutas, *Chem. Phys. Lett.* **404**, 107 (2005).
- <sup>18</sup>J. Blinowski and P. Kacman, *Phys. Rev. B* **64**, 045302 (2001) and references therein.
- <sup>19</sup>M. Björck and G. Andersson, *J. Appl. Cryst.* **40**, 1174 (2007).
- <sup>20</sup>A. Maugert and C. Godart, *Phys. Rep.* **141**, 51 (1986).
- <sup>21</sup>P. Pouloupoulos, S. Baskoutas, S. D. Pappas, C. S. Garoufalis, S. A. Droulias, A. Zamani, and V. Kapaklis, *J. Phys. Chem. C* **115**, 14839 (2011).
- <sup>22</sup>R. M. Xavier, *Phys. Lett. A* **25**, 244 (1967).
- <sup>23</sup>J. D. Axe, *J. Phys. Chem. Solids* **30**, 1403 (1969).
- <sup>24</sup>S. J. Cho, *Phys. Rev. B* **1**, 4589 (1970).
- <sup>25</sup>W. A. Thompson, T. Penny, F. Holtzberg, and S. Kirkpatrick, in *Proceedings of the 11th International Conference on the Physics of Semiconductors* (Polish Scientific, Warsaw, 1972).
- <sup>26</sup>P. Fumagalli, C. Müller, H. Lippitz, and J. J. Paggel, “Array of semiconducting layers for spin injection with high efficiency,” U.S. Patent 6,949,778 (2004).